Poly(glycerol sebacate)\Poly(butylene succinate-dilinoleate) Blends as Candidate Materials for Cardiac Tissue Engineering

M. Tallawi,[1] *R. Rai*,[1] *M. R-Gleixner*,[2] *O. Roerick*,[2] *M. Weyand*,[2] *J. A. Roether*,[3] *D. W. Schubert*,[3] *A. Kozlowska*,[4] *M. El Fray*,[4] *B. Merle*,[5] *M. Göken*,[5] *K. Aifantis*,[6] *A. R. Boccaccini**[1]

Summary: Poly (glycerol sebacate) (PGS) and poly (butylene succinate-dilinoleate) (PBS-DLA) are biodegradable polymers with potential application in cardiac tissue engineering. In the present study novel blends comprising PGS prepolymer and PBS-DLA were prepared with varying compositions (70/30, 60/40, 50/50, 40/60, 30/70 and 0/100 in weight percentage). The physical, chemical, and mechanical properties of the PGS/PBS-DLA blends were measured and compared. By adding PBS-DLA to PGS the need for curing PGS prepolymer was eliminated, as the blended films are chemically stable. With increasing amount of PBS-DLA the hydrophobicity of the blend system increased reaching values close to that of neat PBS-DLA films. Furthermore, addition of PBS-DLA significantly affected the mechanical properties of the blends, i.e. the elastic modulus of the blends was enhanced with increasing PBS-DLA addition from 1.2 MPa to 54 MPa. At the same time, PBS-DLA addition led to decreased degradation rate of the films. Furthermore the PBS-DLA counteracted the acidity of the free carboxylic groups on the free end chains of the PGS prepolymer. *In vitro* cytocompatibility studies indicated high biocompatibility. Taken together the results confirm that the novel PGS/PBS-DLA matrices exhibit promising characteristics as a biomaterial for application in cardiac regeneration approaches.

Keywords: cardiac tissue engineering; mechanobiology; myoblasts; poly (butylene succinate-dilinoleate); substrate stiffness

Introduction

Cardiovascular diseases (CVDs) represents one of the main causes of death as well as a major health problem worldwide and in particular in the western countries.[1] Myocardial infarction (MI) or heart attack, in particular, is one of the major causes of death (30%) amongst all CVDs. MI occurs when the coronary arteries are blocked causing a sudden decrease in blood flow, which leads to a reduction in the supply of oxygen and nutrients in the affected area of the heart muscle.[2–4]

In an adult heart, the damaged tissue cannot be repaired as mature cardiomyocytes have limited capacity to proliferate.[5] Instead, fibrous noncontractile tissue is

[1] Institute of Biomaterials, Department of Materials Science and Engineering, University of Erlangen-Nuremberg, 91058 Erlangen, Germany
E-mail: aldo.boccaccini@ww.uni-erlangen.de
[2] Department of Cardiac Surgery, University of Erlangen-Nuremberg, 91054 Erlangen, Germany
[3] Institute of Polymeric Materials, Department of Materials Science and Engineering, University of Erlangen-Nuremberg, 91058 Erlangen, Germany
[4] Polymer Institute, Division of Biomaterials and Microbiological Technologies, West Pomeranian University of Technology, Szczecin, Poland
[5] Institute of General Materials Properties, Department of Materials Science and Engineering, University of Erlangen-Nuremberg, 91058 Erlangen, Germany
[6] Lab of Mechanics and Materials, School of Engineering, Aristotle University of Thessaloniki, 54124 Thessaloniki, Greece

formed.[6,7] As a viable long-term therapeutic treatment for myocardial infarction, cardiac tissue engineering (CTE) is being investigated.[8,9] In this context, the development of cardiac patches or scaffolds to deliver cells to the infarcted region of the heart is one promising approach.[10]

Cardiac patches are three dimensional (3D) substrates that are fabricated from suitable biodegradable polymers.[10,11] Fundamental properties for a successful scaffold material include biocompatibility, biodegradability and mechanical compatibility with the native myocardium. Cardiac patches serve two main functions, namely they act as carrier of cells and provide mechanical support to the infarcted area.

Many natural, synthetic and composite biomaterials are being investigated as scaffolds or matrix support for cardiac patches.[10,12] Among other biodegradable polymers, the synthetic polyester poly(glycerol-sebacate) (PGS) is attracting increasing interest for cardiac patch applications.[12–16] One reason for selecting PGS is its suitable mechanical properties, biocompatibility and bioresorbability. PGS is prepared by poly-condensing glycerol and sebacic acid.[14] Sebacic acid is the natural metabolic intermediate in ω-oxidation of medium to long-chain fatty acids.[17,18] Glycerol was approved to be used as humectant in foods by the US Food and Drug Administration (FDA).[15] Indeed PGS has been also tested *in vivo* [16,19] and a recent review article has discussed the broad range of PGS applications in the biomedical field.[20] However new investigations about PGS-based materials are required to further improve the biological and mechanical performance of the polymer for cardiac tissue engineering applications.

Poly(butylene succinate-butylene dilinoleate) (PBS-DLA) is a novel multiblock thermoplastic elastomer composed of saturated dilinoleic acid (DLA) as the soft sequence and polybutylene succinate (PBS) as the hard segment. PBS is a promising biodegradable aliphatic polyester.[21] It is a white, highly crystalline polymer, and its main properties are excellent biodegradability, good melt processability (its melting point is at around 115 °C), as well as thermal and chemical resistance. DLA is a flexible chain of butylene ester of dimerised fatty acid.[22]

The synthesised PBS-DLA copolymer has two main transition temperatures (T_g), the low-temperature T_g corresponds to the DLA soft domains and the high-temperature melting transition refers to the PBS crystalline domains, which indicates the two-phase structure of the material. The tensile properties reflect the typical thermoplastic elastomeric behaviour of the copolyester,[23] which combines the strength of engineering plastics with the elasticity of rubber. PBS-DLA also shows a wide range of softness and processing flexibility.[22]

In this study, a range of blends of PGS and PBS-DLA were prepared for the first time and characterized with the aim to study their suitability for use as cardiac patches.

Materials and Methods

PBS-DLA (60/40) with a molecular weight $\sim 50 \cdot 10^3$ g/mol^{-1} was prepared at the Polymer Institute, West Pomeranian University of Technology, Szczecin, Poland. The polymer synthesis was carried out in a 1 dm^3 "pressure-vacuum" reactor. The esterification reaction between DLA, succinic acid and 1,4-butanediol (1,4-BD) was carried out in the presence of magnesium-titanate organometalic complex (Mg-Ti) under intensive stirring and upon programmed temperature raising from 100 °C to 200 °C with a heating rate of 1,5 °C/min. The reaction was finished when acid value less than 2 mg KOH.g-1 was reached. The polycondensation reaction was carried out at 245–250 °C, ~0,4 hPa and in the presence of Mg-Ti catalyst. The process was considered complete when the observed power consumption of the stirrer motor signaled that the polymer of highest melt viscosity was obtained. The reaction mass was extruded by means of compressed nitrogen. The copolyester was purified

dissolving the polymer in chloroform and precipitating in methanol. PBS-DLA was synthesized to produce random copolymer containing 60 wt% of PBS segments and 40 wt% of DLA segments, respectively.

PGS Preparation

For the synthesis of PGS, commercially purchased sebacic acid and glycerol (Sigma-Aldrich, Germany) were used. PGS was synthesized according to the technique proposed by Wang *et al.*[14] The synthesis of PGS normally involves two steps; pre-polycondensation step and crosslinking. For the pre-polycondensation step, an equimolar mixture (0.1 M) of glycerol and sebacic acid was heated at 120 °C under inert nitrogen atmosphere to form the pre-polycondensed polymer. The pre-polycondensed polymer was a transparent viscous like gel. PGS in this study was used in the prepolymer condition without further crosslinking.

Fabrication of Two Dimensional (2D) PGS/PBS-DLA Matrices by Solvent Casting

The fabrication of PGS/PBS-DLA matrices was carried out by solvent casting. Films were fabricated by dissolving the two polymers (PGS and PBS-DLA) in dichloromethane (DCM) for 2 hours, then casting the solution in a covered glass petri dish (70 mm diameter). The films were left to dry in air for two days and then they were freeze dried for 1 day followed by ethanol (70%) treatment for 24 hours. The ethanol treatment leaches out any free or unreacted monomers and it should also remove any remaining of solvent. The final cast PGS/PBS-DLA films had thickness of 0.5 mm and were 70 mm in diameter. The thicknesses of the films were controlled by using a fixed volume of the polymer. To study the effect of PBS-DLA addition to PGS, 7 samples were prepared, with the following PGS/PBS-DLA weight ratios: 100/0, 70/30, 60/40, 50/50, 40/60, 30/70 and 0/100.

In Vitro Degradation Study

In vitro degradation studies of the different PGS/PBS-DLA films (n = 3) were carried out in phosphate buffer saline (PBS) medium for periods of 1, 3, 7, 14, 21 and 28 days. The samples used were 3 cm in length and 0.5 cm in width. The degradation kinetics of the fabricated films was determined by measuring the % water uptake or absorption (% WA) and the % weight loss (% WL). The samples were first weighed to obtain the dry weight $M0_{dry}$, ($M0_{dry}$ is the initial weight of the sample), immersed in 20 ml of PBS-saline solution, incubated at 37 °C and 90 rpm. At each incubation time point the films were analysed for weight loss (% WL) behavior. The pH of the supernatant was also measured at each incubation time point. For measuring the % WL, the samples were withdrawn from the PBS solution, washed several times with deionized water and dried at 37 °C overnight. Subsequently they were weighted dry to obtain Mt_{dry} (Mt_{dry} is the dry weight of the samples after immersion in the PBS solution followed by drying). The weight loss was calculated using equation 1:

$$\%\,\mathrm{WL} = [(\mathrm{Mo}_{dry} - \mathrm{Mt}_{dry})/\mathrm{Mo}_{dry}] * 100 \quad (1)$$

In Vitro Cytocompatibility Studies

A mouse skeletal myoblast cell line (C2C12; CRL-1772, ATTC, Rockville, Maryland, USA) was cultured with concentration of 10^4 cells/ml in RPMI containing 1% penicillin/streptomycin, 2 mM L-glutamine (Sigma-Aldrich) and 10% v/v fetal bovine serum (Sigma-Aldrich) maintained at 37 °C and 5% CO_2. Cells were passaged every third day using a solution containing 0.25% trypsin/1mM ethylenediaminetetraacetic acid (EDTA; Nacalai Tesque Inc., Kyoto, Japan). The medium was changed every day throughout the entire experiment and the samples were processed after 3, 8, 24 and 72 hours for immunofluorescence analysis. WST-8 was used to measure cell metabolic activity quantitatively after 3, 8, 24 and 72 hours of direct cell culturing. Thus, the assay was used to evaluate cell adhesion and proliferation on the developed matrices as an indirect measurement of cell activity. The cell morphology and the formation of adhesion processes were

detected via scanning electron microscopy (SEM) and immunofluorescence staining using Phalloidin and DAPI to visualize the cytoskeleton organization and cell nucleus, respectively.

Immunofluorescence Staining and Microscopy

Cells seeded on PGS/PBS-DLA matrices were fixed with 4% PFA in PBS for 15 min at room temperature and permeabilized with 0.1% Triton X-100 (Sigma-Aldrich) in PBS for 15 min at room temperature after 3, 8, 24 and 72 in hours culture. C2C12 cell morphology, cytoskeleton organization and protein expression were detected through immunofluorescence analysis after incubation with Alexa Fluor®555 Phalloidin (1:60; Invitrogen), a drug directed against F-actin, for 1 h at room temperature. Nuclei were counterstained with 4–6-diamidino-2-phenylindole (DAPI; Sigma-Aldrich).

Characterisation of PGS/PBS-DLA Films

Chemical Structure Assessment via Attenuated Total Reflectance-Fourier Transform Infrared (ATR-FTIR) spectroscopy

Chemical analysis of the polymeric films was carried out in attenuated total reflectance mode (ATR) of the FTIR spectrometer (Nicolet 6700, Thermo Scientific Germany). The penetration depth was 2–3 μm. The analyses were performed under the following conditions: Spectral range between, 4000 to 530 cm^{-1}; window material, CsI: 64 scans at a resolution of 4 cm^{-1}.

Surface Analysis

To study the surface morphology of different PGS/PBS-DLA matrices and to demonstrate the effect of PBS-DLA on the surface morphology a LEO 435 VP scanning electron microscope was used. Samples were prepared by placing them on 8 mm diameter aluminium stubs, which were sputtered with gold with 2% palladium. The SEM images were captured at an acceleration voltage of 5 kV.

The wettability of the scaffolds was evaluated using static contact angle measurements. The reference liquid was deionized water (3 μl), and was placed on every sample by means of a gas tight microsyringe forming a drop. Photos (frame interval: 1 s, number of frames; 100) were taken to record the shape of the drops. The water contact angles on the specimens were measured by analysing the recorded drop images using the Windows based KSV CAM software. Five repeats of each reference liquid for each sample were carried out. The experiment was done on a KSV CAM 200 optical contact angle meter (KSV Instruments Ltd).

Atomic force microscopy (AFM) measurements were performed with a Dimension 3100 Atomic Force Microscope (Bruker, USA). The samples were investigated using NSG-10 probes (NT-MDT, Russia) in intermittent contact mode. This experiment allowed gathering quantitative information about the topography and enabled to qualitatively show phase separation.

Mechanical Properties

Tensile tests were carried out using a Zwick Universal Testing Machine Z050 at room temperature. The samples were cut into rectangular strips that were 5 mm wide, 3 cm long and 0.5 mm thick. The measurements were carried out at a crosshead speed of 10 mm/min and a pretension of 0.2 N was applied. A 50 N load cell was used for all experiments.

Statistical Analysis

The data sets ($n = 3$) have been expressed along with their mean standard deviation. The data, where appropriate, were compared using the one way ANOVA and differences were considered to be significant when $^{*}p < 0.05$.

Results and Discussion

An in depth investigation was carried out to characterize various properties of PGS/

PBS-DLA blends, such as structural, microstructural, surface physiochemical and thermal behaviour.

Structural Characterization

To determine the successful fabrication of PGS\PBS-DLA blends preliminary structural characterization was done by studying the ATR-FTIR signature spectra of the polymers. Figure 1 shows the FTIR spectra of the different PGS\PBS-DLA blends. The results confirm the presence of the characteristic marker corresponding to both PGS and PBS-DLA. Ester carbonyl band which occurs at 1 731 and 1 742 cm^{-1} and the band at 1 165 cm^{-1} correspond to CO stretching for both PGS and PBS-DLA.[24] The bands at 2 925 and 2 856 cm^{-1} correspond to the aliphatic CH group of the polymer backbone. [25] The bands between 1 364 and 1 450 cm^{-1} occur due to CH_3 stretching. All the PGS and PBS-DLA peaks in the blends overlap except for the peak at 980 cm^{-1} which corresponds to the PBS-DLA and the peak at 3 400 cm^{-1} for the hydroxyl groups which indicates the presence of PGS. The intensity of this peak increased with increasing amount of PGS in the blends.

Microstructural Studies

Surface and microstructural features of a biomaterial can have important implications on its biocompatibility, the rate of cell attachment and proliferation and hence its applications. Therefore, to evaluate these microstructural properties and understand their impact on the biocompatibility, the fabricated films were subjected to a series of tests using SEM, AFM phase scan and contact angle measurements.

The surface morphology and microstructure of these films were observed by SEM and AFM. SEM micrographs revealed increased surface roughness with increasing content of PBS-DLA (figure 2A-F). The neat PBS-DLA revealed very rough surface properties, with a kind of microbead

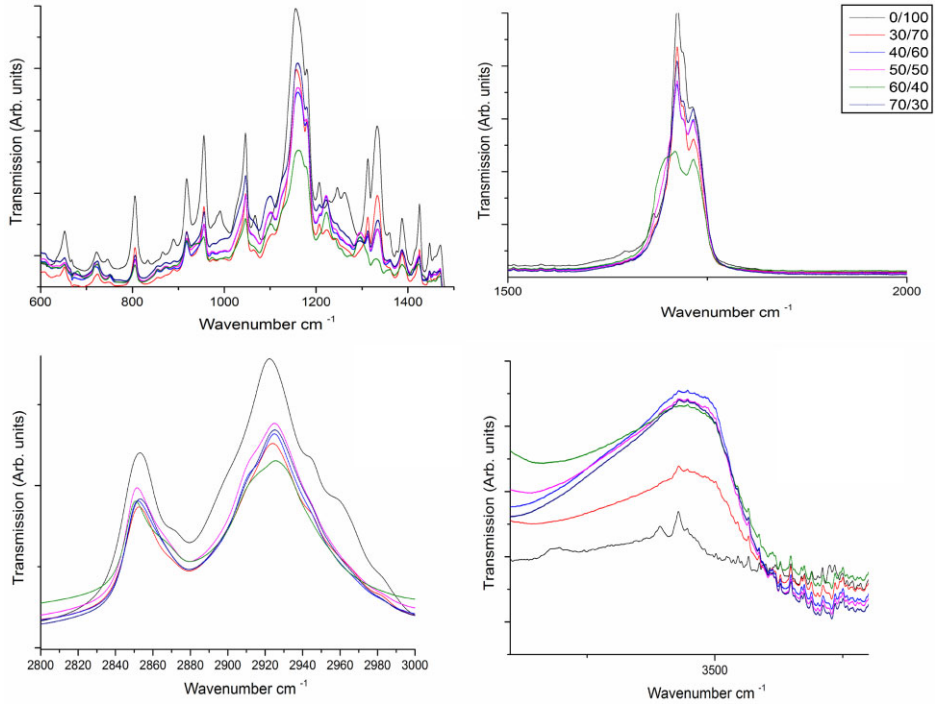

Figure 1.
ATR-FTIR spectra of different PGS/PBS-DLA blends.

structure as observed in Figure 2F. On the other hand, the SEM micrograph of the neat PGS shows a smooth surface as shown in Figure 2A. From the SEM micrographs, it can be seen that the microbead structure of the PBS-DLA gradually becomes more prominent with increasing amounts of PBS-DLA.

AFM scanning was performed on PGS/PBS-DLA films to investigate their topography in detail. These experiments were performed in intermittent contact mode. In addition to the topography data, a phase signal was also obtained revealing the areas of different compositions (in the PGS/PBS/DLA blends). Usually the signal depends on several parameters such as elasticity, friction and adhesion. The AFM data demonstrated that the film surfaces become smother as the PGS content in the blend increases with surface roughness (R_a) values of 2.2, 1.9, 1,5, 1.1, 0.7 and 0.8 μm for PGS/PBS-DLA 0/100, 30/70, 40/60, 50/50, 60/40 and 70/30, respectively.

Figure 3 shows the AFM phase scan revealing a phase separation behavior and nonhomogeneous blends between PGS and PBS-DLA in most of the samples (except for the PGS/PBS-DLA 40/60), which demonstrates that PGS and PBS-DLA are not well miscible.

Water contact angle measurements were carried out on the surfaces of the blend films to assess their wettability. The water contact angle (θ_{H2O}) is a measure of the hydrophilicity or hydrophobicity of a material surface. Surfaces with θ_{H2O} less than 70 ° are considered to be hydrophilic and θ_{H2O} greater than 70 ° are measured on hydrophobic surfaces.[26] Figure 4 demonstrates the effect of PBS-DLA content on the water contact angle. The hydrophobicity of the blend system increased with increasing content of PBS-DLA, i.e. a PBS-DLA film exhibits an average contact angle of between 80 ° and 114 ° depending on whether the smooth or rough side was tested whereas with increasing PGS content the blends are in the hydrophilic range. However, the wettability of the fabricated matrices was possibly also affected by the increasing surface roughness due to the increase in PBS-DLA content as confirmed by SEM and AFM studies. Furthermore, the wettability of the films was different when measured on both sides of the films, showing higher values on the upper (rough) side of the films compared to the bottom (smooth) side, which confirms the influence of the surface roughness on the wettability.

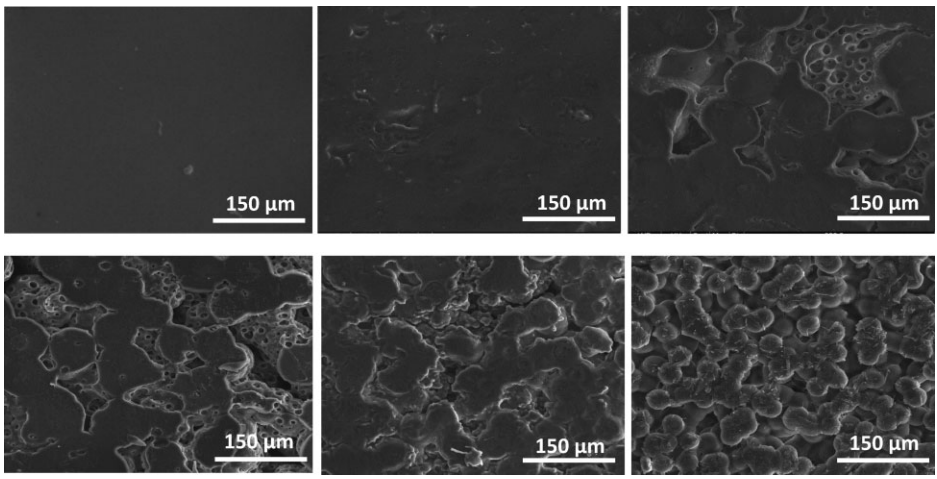

Figure 2.
SEM micrographs of PGS/PBS-DLA blends of different concentrations; A: PGS: 100/0, B: 70/30, C: 60/40, D: 50/50, E: 40/60, F: 0/100.

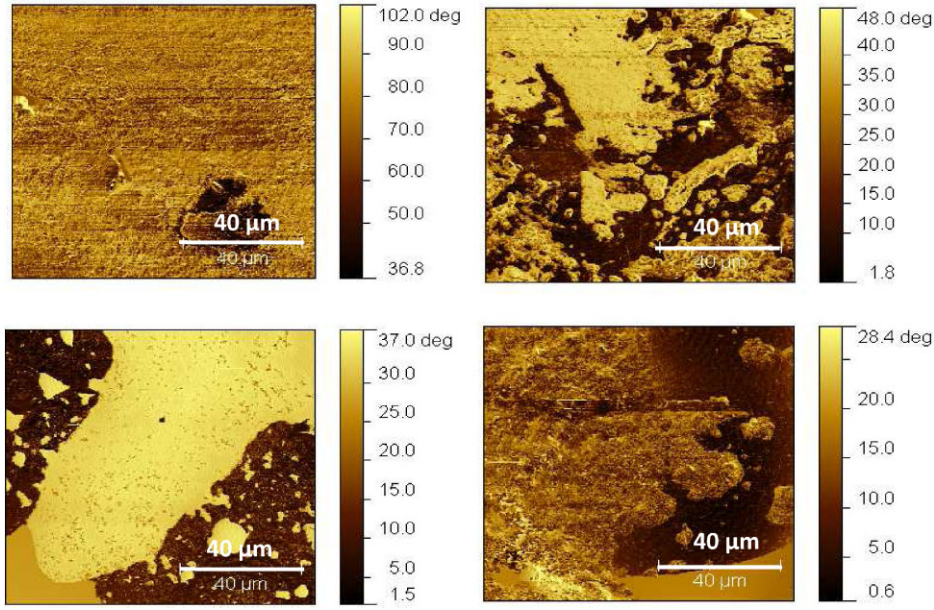

Figure 3.
AFM phase scan micrographs of PBS-DLA blends, A: 40/60 B: 50/50; C 60/40; D: 70/30.

Mechanical Properties

Static conventional tensile strength tests were carried out on the fabricated PGS/PBS-DLA films to understand their mechanical properties. The stress strain curves of the neat films of PGS and PBS-DLA are shown in Figure 5. The stress strain curve observed for all the samples resembled that of elastomers. A knee (yield point) i.e., the point of discontinuity in the slope of the stress strain-curve, is not observed in any of the curves (see figure 5).[27] The Young's modulus values calculated from the slope of the curves for the different PGS/PBS-DLA blends are summarized in Table 1. The Young's modulus increased as the PBS-DLA content increased reaching that of neat PBS-DLA (54 MPa).

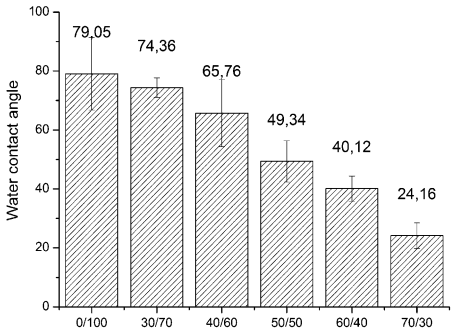

Figure 4.
Water contact angle values for the different PGS/PBS-DLA blends.

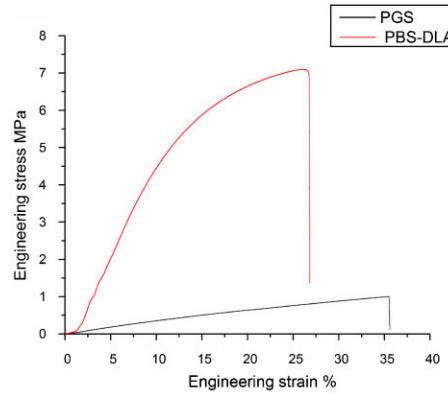

Figure 5.
Stress-strain curves of PGS/PBS-DLA 100/0 (neat PGS) and 0/100 (neat PBS) films.

Table 1.
Mechanical properties of PGS/PBS-DLA matrices of different compositions.

Sample	0\100	30\70	40\60	50\50	60\40	70\30	100/0
Young's modulus (MPa)	54 ± 2	34 ± 2	28 ± 3	26 ± 2	14 ± 3	10 ± 3	1.2
Stress at failure (MPa)	7.5 ± 1.1	2.7 ± 0.2	1.4 ± 0.1	1.9 ± 0.1	1.8 ± 0.5	1.8 ± 0.2	0.8 ± 0.1
Strain at failure (%)	29.2 ± 2.6	20.1 ± 0.1	10.2 ± 1.0	20.3 ± 1.3	19.6 ± 1.0	21.1 ± 0.1	28.7 ± 5.5

In Vitro Degradation Study

A detailed study on the *in vitro* degradation behaviour of the fabricated PGS/PBS-DLA films was carried out by thermostatically incubating the fabricated films at 37 °C up to a period of 28 days in PBS solution. The % weight lost (WL) during degradation of the films was calculated as a percentage of weight loss from the original weight of the film. The % WL of the films is depicted in Figure 6 A. The results show that the weight loss of the films increased progressively with incubation time, as expected.

Furthermore the maximum weight loss observed at 28 days is 12.8 ± 0.8% and 3.2 ± 0.2% for the 60/40 and 0/100 films, respectively. The media in which the matrices were incubated for the degradation study were monitored to analyse possible pH changes owing to the degradation products of the polymers. The results of the pH study are shown in Figure 6 B. The pH of the media was seen to decrease as degradation progressed. The pH was and 6.7 ± 0.1 and 7.5 ± 0.1 at 28 days for PGS/PBS-DLA 60/40 and 0/100 respectively. The pH decreased because of acidification of the medium by ionization of unreacted carboxylic acid groups during the degradation of the polymers. The degradation kinetics of the PGS/PBS-DLA 60/40, decreased drastically compared to that of PGS/PBS-DLA 0/100. Both films exhibit linear degradation kinetics over the different incubation periods confirming a surface degradation dominated behaviour.

In Vitro Cell Studies

Substrate stiffness has been shown to affect cell behavior in terms of survival, proliferation and differentiation,[28–31] while the response of cells to matrix elasticity *in vitro* has been demonstrated to be highly cell specific.[32,33] To investigate the possibility that matrix compliance could interfere with myoblast function, the substrate stiffness has been modulated by incorporating

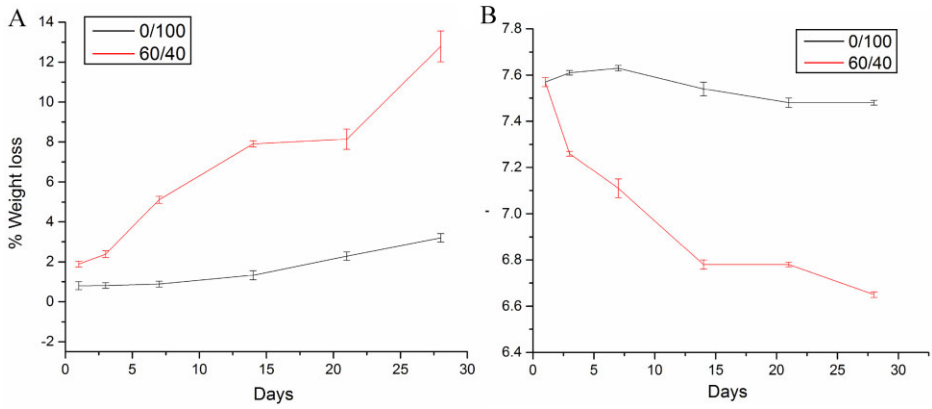

Figure 6.
A: % weight loss of the degrading PGS/PBS-DLA blends during *in vitro* degradation study in PBS; B: pH-values of the media (PBS) in which the PGS/PBS-DLA 60/40 and 0/100 films were incubated for the *in vitro* degradation study. The pH of the medium was measured at each time point.

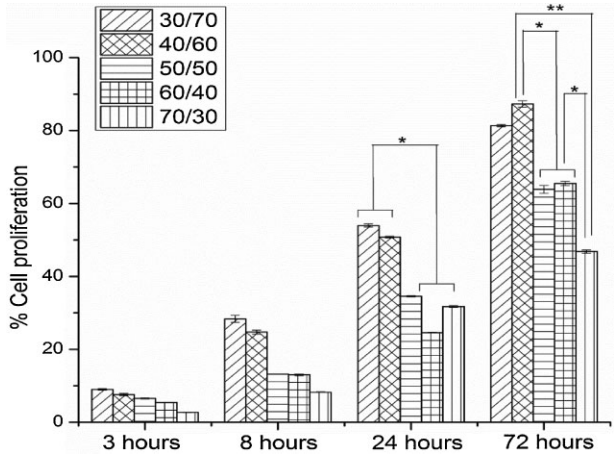

Figure 7.
Percentage C2C12 cell proliferation over different time points (3, 8, 24, 72 hours). Cell proliferation was normalized to tissue culture plate (positive control), showing the highest cell viability for the 40/60 (28 ± 3 MPa) samples. The data ($n = 3$; error bars $= \pm$ SD) were compared using the one way ANOVA and differences were considered significant when $^{*}p < 0.05$.

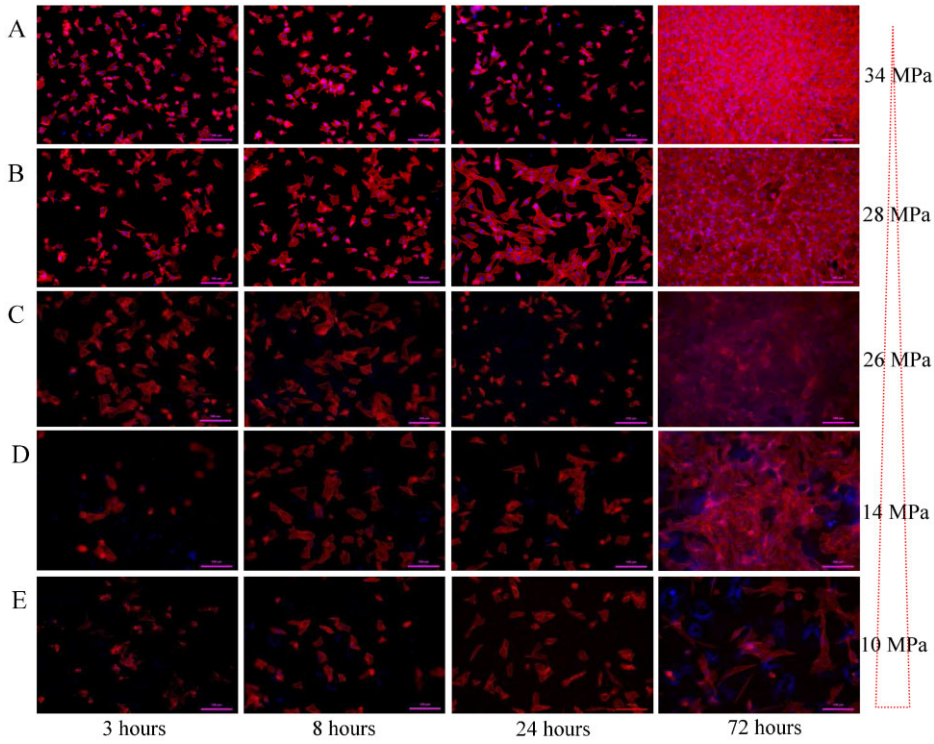

Figure 8.
C2C12 cells were cultured on PGS/PBS-DLA matrices of different stiffness. Cell morphology and the formation of adhesion processes were detected by immunofluorescence staining after 8h, 24h and 72h of culture, A: 30/70, B: 40/60, C: 50/50, D: 60/40, E: 70/30. To visualize the cytoskeleton organization, F-actin was decorated by Alexa Fluor® 555 Phalloydin (red). (Scale bar (▬) = 100 μm).

PBS-DLA to PGS prepolymer. PGS/PBS-DLA matrices were produced with overall Young's modulus of 34 ± 2 MPa, 28 ± 3 MPa, 26 ± 2 MPa, 14 ± 3 MPa and 10 ± 3 MPa for PGS/PBS-DLA 30/70, 40/60, 50/50, 60/40 and 70/30 samples, respectively, as seen in Table 1.

Cell viability studies performed with C2C12 revealed no significant differences in myoblast cell adhesion after 3 hours of seeding (Figure 7). Interestingly, 72 h after seeding, the seeded cells exhibited a typical myoblast-like morphology on all substrates, showing a correct cytoskeleton organization highlighted by F-actin immunostaining, irrespective of the substrate stiffness and confirmed by SEM analysis (Figure 8). These data demonstrate the effect of substrate elasticity on myoblast cells in short-term investigations. In addition, it was observed that the cells proliferated to a higher extent on the stiffer substrates as shown in Figure 7.

Both the immunostaining and SEM micrographs (see figure 8 and 9) confirm the cell viability data, where the cells proliferated to a higher extent on the stiffer (higher PBS-DLA content) matrices. Figure 9 shows the spreading of cells all over the surface after 72 hour of seeding. A film of cells on the stiffer matrices has formed compared to the softer samples on which very few cells even after 72 hours of culture are seen. Furthermore the cells on the stiffer substrate seem to be more stretched than those on the softer substrate (see figure B 2 and 4).

The stiffness is not however the only factor affecting the cell behavior; indeed, the surface chemistry affects cell adhesion and proliferation. This approach has thus shown the difficulty in controlling the surface wettability in the present blend system. In addition, the surface roughness was found to increase with increasing amounts of PBS-DLA, which, in turn, plays an important role in cell adhesion.

Conclusion

A variety of blend compositions composed of PGS and PBS-DLA were fabricated and analysed. The study demonstrated that the PBS-DLA addition to PGS enabled tailoring the mechanical properties of the blends to a great extent, leading to increase of the Young's modulus, while PBS-DLA addition decreased the degradation rate and increased the surface roughness. The nature of the matrix affects cell behavior and matrix stiffness appears to be a critical parameter as the stiffer films containing higher degrees of PBS-DLA also showed the highest proliferation of C2C12 cells. Nevertheless, there are other factors that contribute to cell behavior, such as surface chemistry (different hydrophilicity), surface roughness and biological factors, all which require further attention for the complete

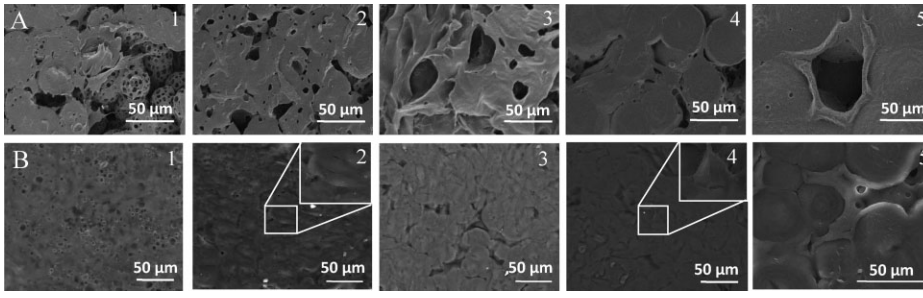

Figure 9.
Details of the focal adhesion processes are shown in the SEM micrographs after A: 24 h and B: 72 h for the 30/70, 40/60, 50/50, 60/40, 70/30 films, respectively, confirming the morphology of adherent cells and showing the spreading of the cells on the surface after 72 hour of seeding.

optimization of PGS/PBS-DLA polymers for cardiac patch applications.

Acknowledgements: Funding from ERC project MINATRAN is acknowledged.

[1] WHO. **2010** [cited; Available from http://www.greenerpackage.com/bioplastics/biodegradable_polymers_market_grow_13_through_2014
[2] R. N. Kitsis, J. Narula, *Heart fail Rev.* **2008**, *13*, 107.
[3] N. G. Frangogiannis, M. L. Entman, *Circulation* **2004**, *110*, 1341.
[4] R. M. Moura, A. A. de Queiroz, *Artif Organs* **2011**, *35*, 471.
[5] J. Kajstura, N. Gurusamy, B. Ogòrek, P. Goichberg, C. Clavo-Rondon, T. Hosoda, D. D'Amario, S. Bardelli, A. P. Beltrami, D. Cesselli, R. Bussani, F. del Monte, F. Quaini, M. Rota, C. A. Beltrami, B. A. Buchholz, A. Leri, P. Anversa, *Circ Res.* **2010**, *107*, 1374.
[6] F. Quaini, E. Cigola, C. Lagrasta, G. Saccani, E. Quaini, C. Rossi, G. Olivetti, P. Anversa, *Circ Res.* **1994**, *75*, 1050.
[7] J. Kajstura, N. Gurusamy, B. Ogòrek, P. Goichberg, C. Clavo-Rondon, T. Hosoda, D. D'Amario, S. Bardelli, A. P. Beltrami, D. Cesselli, R. Bussani, F. del Monte, F. Quaini, M. Rota, C. A. Beltrami, B. A. Buchholz, A. Leri, P. Anversa, *Circ Res* **2010**, *107*, 1374.
[8] M. W. Curtis, B. Russell, *J Cardiovasc Nurs.* **2009**, *24*, 87.
[9] A. R. Boccaccini, S. Harding, "*Myocardial Tissue Engineering*", Springer, **2011**.
[10] H. Jawad, N. N. Ali, A. R. Lyon, Q. Z. Chen, S. E. Harding, A. R. Boccaccini, *J Tissue Eng Regen Med* **2007**, *1*, 327.
[11] A. A. Rane, K. L. Christman, *J Am Coll Cardiol* **2011**, *58*, 2615.
[12] Q. Z. Chen, A. Bismarck, U. Hansen, S. Junaid, M. Q. Tran, S. E. Harding, N. N. Ali, A. R. Boccaccini, *Biomaterials* **2008**, *29*, 47.
[13] J. M. Kemppainen, S. J. Hollister, *J Biomed Mater Res A* **2010**, *94*, 9.
[14] Y. Wang, G. A. Ameer, B. J. Sheppard, R. A. langer, *Nat Biotechnol.* **2002**, *20*, 602.
[15] J. R. Venugopal, M. P. Prabhakaran, S. Mukherjee, R. Ravichandran, K. Dan, S. Ramakrishna, *J R Soc Interface* **2012**, *9*, 1.
[16] Q. Z. Chen, S. E. Harding, N. N. Ali, A. R. Lyon, A. R. Boccaccini, *Material Science and Engineering R* **2008**, *59*, 1.
[17] G. Liu, B. Hinch, A. D. Beavis, *J Biol Chem* **1996**, *271*, 25338.
[18] P. B. Mortensen, *Biochim Biophys Acta* **1981**, *664*, 349.
[19] J. Tamada, R. Langer, *J Biomater Sci Polym Ed* **1992**, *3*, 315.
[20] R. Rai, M. Tallawi, A. Grigore, A. R. Boccaccini, *Progress in Polymer Science* **2012**, *37*, 1051.
[21] E. Rudnik, "*Compostable Polymer Material*", Elsevier, **2010**, 28.
[22] A. Kozlowska, D. Gromadzki, M. El Fray, P. Štěpánek, *FIBRES & TEXTILES in Eastern Europe* **2008**, *16*, 85.
[23] M. El Fray, V. Altstädt, *Polymer* **2003**, *44*, 4635.
[24] S. Randriamahefa, E. Renard, P. Guerin, V. Langlois, *Biomacromolecules* **2003**, *4*, 1092.
[25] R. Sánchez, J. Schripsema, L. F. da Silva, M. K. Taciro, G. C. Pradella, G. C. Gomez, *European Polymer Journal* **2003**, *39*, 1385.
[26] G. Peschel, H. M. Dahse, A. Konrad, G. H. Wieland, P. J. Mueller, D. P. Martin, M. Roth, *J Biomed Mater Res* **2007**, 1073.
[27] L. Nocolais, R. A. Mashelkar, *International Journal of Polymeric Materials* **1977**, *5*, 317.
[28] A. J. Engler, S. Sen, H. L. Sweeney, D. E. Discher, *Cell* **2006**, *126*, 677.
[29] G. Forte, F. Carotenuto, F. Pagliari, *Stem Cells* **2008**, *26*, 2093.
[30] A. Leal-Egaña, A. Díaz-Cuenca, A. R. Boccaccini, *Adv. Mater.* **2013**, in press.
[31] G. Forte, *Tissue Eng Part A* **2012**, *18*, 1837.
[32] P. C. Georges, P. A. Janmey, *J. Appl Physiol* **2005**, *98*, 1547.
[33] I. Banerjee, K. Yekkala, T. K. Borg, T. A. Baudino, *Ann N Y Acad Sci* **2006**, *76*, 1080.

